Published in final edited form as:
Clin Cancer Res. 2010 October 1; 16(19): 4779–4788. doi:10.1158/1078-0432.CCR-10-1818.

PRECLINICAL CHARACTERIZATION OF MITOCHONDRIA-TARGETED SMALL MOLECULE Hsp90 INHIBITORS, GAMITRINIBS, IN ADVANCED PROSTATE CANCER

Byoung Heon Kang[1,2,4], **Markus D. Siegelin**[1,2], **Janet Plescia**[1,2], **Christopher M. Raskett**[1,2], **David S. Garlick**[2], **Takehiko Dohi**[1,2], **Jane B. Lian**[1,3], **Gary S. Stein**[1,3], **Lucia R. Languino**[1,2], and **Dario C. Altieri**[1,2]

[1]Prostate Cancer Discovery and Development Program, University of Massachusetts Medical School, Worcester, MA 01605

[2]Department of Cancer Biology, University of Massachusetts Medical School, Worcester, MA 01605

[3]Department of Cell Biology, University of Massachusetts Medical School, Worcester, MA 01605

Abstract

Purpose—To characterize the preclinical activity of the first class of combinatorial, mitochondria-targeted, small molecule Hsp90 inhibitors, Gamitrinibs, in models of hormone-refractory, drug-resistant and localized and bone metastatic prostate cancer, in vivo.

Experimental design—Mitochondrial permeability transition, apoptosis and changes in metabolic activity were examined by time-lapse videomicroscopy, multiparametric flow cytometry, MTT and analysis of isolated mitochondria. Drug-resistant prostate cancer cells were generated by chronic exposure of hormone-refractory PC3 cells to the Hsp90 inhibitor, 17-allylaminogeldanamycin (17-AAG). The effect of Gamitrinibs on subcutaneous or intratibial prostate cancer growth was studied in xenograft models. Bone metastatic tumor growth and bone parameters were quantified by μCT imaging.

Results—In the NCI 60-cell line screening, Gamitrinibs were active against all tumor cell types tested, and efficiently killed metastatic, hormone-refractory and multidrug-resistant prostate cancer cells characterized by over-expression of the ATP Binding Cassette (ABC) transporter, P-glycoprotein. Mechanistically, Gamitrinibs, but not 17-AAG, induced acute mitochondrial dysfunction in prostate cancer cells with loss of organelle membrane potential, release of cytochrome c, and caspase activity, independently of pro-apoptotic Bcl-2 proteins, Bax and Bak. Systemic administration of Gamitrinibs to mice was well tolerated, and inhibited subcutaneous or bone metastatic prostate cancer growth, in vivo.

Conclusions—Gamitrinibs have preclinical activity and favorable safety in models of drug-resistant and bone metastatic prostate cancer, in vivo.

Keywords

Prostate cancer; bone metastasis; mitochondria; Hsp90; drug resistance

Correspondence: Dario C. Altieri, M.D., Department of Cancer Biology, LRB428, 364 Plantation Street, Worcester, MA 01605, Tel. (508) 856-5775; FAX (508) 856-5792; dario.altieri@umassmed.edu.
[4]Present address: School of Nano-Biotechnology & Chemical Engineering, Ulsan National Institute of Science and Technology (UNIST), 100 Banyeon-ri, Ulsan, 689-798 South Korea

DISCLOSURE OF POTENTIAL CONFLICT OF INTEREST
No potential conflicts of interest were disclosed.

INTRODUCTION

Despite advances in the treatment of early phase prostate cancer (1), the management of advanced, castration-resistant and bone metastatic disease remains challenging (2), with high morbidity, poor quality of life, and over 30,000 deaths from disease in the US alone. There are few therapeutic options for these patients, as mainstay cytotoxic and radiation are only partially effective, and emerging molecular therapies have yet to show meaningful prolongation of survival (3).

Among the molecular changes that characterize advanced prostate cancer (4) is an intrinsic resistance to apoptosis (5), especially mitochondrial cell death (6). This process involves a cascade of molecular changes, including loss of organelle transmembrane potential, swelling of the matrix, and rupture of the outer membrane, culminating with the discharge of apoptogenic proteins, most notably cytochrome c, in the cytosol (7). Regulators of such "mitochondrial permeability transition" (8), for instance, anti-apoptotic Bcl-2 proteins controlling outer membrane integrity (9), have been intensely pursued for novel molecular therapeutics of advanced prostate cancer. However, the suitability of other, "mitochondrial-intrinsic" cytoprotective mechanisms as novel therapeutic targets in prostate cancer is only recently beginning to emerge (10).

Potential candidates for this pathway (10) are the molecular chaperones of the Heat Shock Protein (Hsp) family (11), including Hsp90 and its related chaperone, TNF Receptor-Associated Protein-1 (TRAP-1). Abundantly expressed in mitochondria of tumor cells (12), including all Gleason grade localized and metastatic prostate cancer, but not normal prostatic epithelium, in vivo (13), Hsp90 chaperones associate with Cyclophilin D (CypD) (12), a component of the organelle permeability transition pore (7), and antagonize its function, preserving mitochondrial integrity and shutting off the initiation of cell death (12).

In this context, Hsp90 has long been recognized as an attractive "nodal" target for cancer therapy, intersecting multiple, downstream pathways of cell proliferation, survival and adaptation required for tumor progression. However, despite the promise of simultaneous multiple pathway inhibition in tumors, Hsp90-based therapy (14) has shown so far modest activity in the clinic, often compromised by significant toxicity. Intriguingly, none of the structurally diverse small molecule Hsp90 antagonists in (pre)clinical development (15) accumulates in mitochondria, raising the possibility that inhibition of this compartmentalized pool of the chaperone may be required for optimal Hsp90-directed therapy (16).

In this study, we tested the preclinical activity of Gamitrinibs (GA mitochondrial matrix inhibitors), the first class of combinatorial, mitochondria-targeted Hsp90 inhibitors (16) in models of advanced prostate cancer. Compared to non-subcellularly targeted Hsp90 inhibition, Gamitrinibs act as direct "mitochondriotoxic" agents in prostate cancer, triggering irreversible organelle dysfunction, tumor cell death and inhibition of superficial and bone localized prostate cancer growth, in vivo.

MATERIALS AND METHODS

Cell culture and antibodies

Metastatic prostate cancer PC3 and normal prostatic epithelial BPH-1 cells were obtained from the American Type Culture Collection (ATCC, Manassas, VA), and maintained in culture according to the manufacturer's instructions. Androgen-independent and metastatic prostate cancer C4-2B cells were described previously (17). To develop drug resistance, PC3 cells were cultivated in complete growth medium containing 17-AAG (up to 5 μM) for 4–6 mo. The

surviving cell type, designated PC3-GA, was selected for additional studies. The following antibodies to Hsp90 (BD Biosciences), Hsp27 (Cell Signaling), TRAP-1 (BD Biosciences), Hsp60 (BD Biosciences), cytochrome c (Clontech), COX-IV (Clontech), β-actin (Sigma-Aldrich), Bax (CST Inc., Danvers, MA), Bak (CST), c-Src (Santa Cruz), Tyr416-phosphorylated Src (p-Src) (Biosource International), and Akt (Cell Signaling), were used.

Chemicals

The complete chemical synthesis, HPLC profile, and mass spectrometry of mitochondria-targeted small molecule Hsp90 antagonists, Gamitrinibs (GA mitochondrial matrix inhibitors), have been reported previously (16). The structure of Gamitrinibs is combinatorial and contains the Hsp90 ATPase inhibitory structure of 17-AAG (LC-Laboratories, Woburn, MA) linked to 1 to 4 repeats of guanidinium (Gamitrinib-G1–G4, G-G1–G4), or triphenylphosphonium (Gamitrinib-TPP, G-TPP), used as structurally different mitochondriotropic moieties (16).

Mitochondrial isolation

Mitochondrial extracts were isolated from PC3 or BPH-1 cells using a Mitochondria Isolation kit for cultured cells (PIERCE), as described (12). Briefly, cultured cells were washed in TD buffer (135 mM NaCl, 5 mM KCl, 25 mM Tris, pH 7.6), and cell pellets in CaRSB buffer (10 mM NaCl, 1.5 mM $CaCl_2$, 10 mM Tris, pH 7.5 plus protease inhibitors) were homogenized in a Dounce grinder and immediately mixed with MS buffer, and processed as described (18). Crude mitochondrial fractions were collected by centrifugation at 6,000 g for 10 min, and suspended in MS buffer containing 210 mM mannitol, 70 mM sucrose, 5 mM Tris, pH 7.6, 5 mM EDTA, and protease inhibitors. Samples were incubated with increasing concentrations of G-TPP (0.8–20 μM) or 17-AAG (4–20 μM) for 30 min and analyzed for changes in cytochrome c content in pellets or supernatants, by Western blotting. Protein concentrations were determined with a Protein Assay reagent (BioRad) using BSA (Sigma-Aldrich) as standard.

Mitochondrial membrane potential

Mitochondria isolated from PC3 cells (100 μg) were suspended in SB buffer and incubated with 0.1 μM tetramethylrhodamine methyl ester (TMRM), treated with G-TPP (0.4 μM), G-G4 (0.4 μM), or 17-AAG (1.5 μM), in the presence or absence of the CypD inhibitor, cyclosporine A (CsA, 5 μM), and analyzed continuously for changes in fluorescence intensity at 549 nm excitation and 575 nm emission (Photon Technology International, Inc), as described (12). TMRM-loaded mitochondria in SB buffer were allowed to reach stable fluorescence, which was set as fully polarized state. The fluorescence intensity after treatment with 2 mM $CaCl_2$ was set as minimum membrane potential (fully depolarized state). Changes in fluorescence intensity were plotted as a ratio between maximum and minimum membrane potential.

In some experiments, PC3 cells (10^5) were plated on optical-grade 35 mm glass bottom tissue culture dishes and labeled with MitoTracker green (200 nM) for 16 h at 37°C. After washes, cells were incubated with fresh media in the presence of 100 nM TMRM (red fluorescence) for 30 min, and then with 40 nM TMRM. After treatment with G-TPP (30 μM), individual cells (average, 6–10 cells per field) were imaged continuously on a Nikon TE2000-E2 with a Perfect Focus System inverted microscope using a CSU10B Spinning Disk Confocal System. Images were acquired every 5 min by time lapse videomicroscopy on a Rolera Mgi EMCCD camera in an environmental chamber (20/20 Technology) using a 60× objective, and quantified for real-time kinetics of changes in mitochondrial membrane potential.

Transfections

PC3 cells were simultaneously transfected with Bax- and Bak-directed SMARTPool small interfering RNA (siRNA) (Dharmacon cat. n. L-003308-01-0005, L-003305-00-0005) using Oligofectamine 2000, and characterized for protein knockdown by Western blotting.

Analysis of cell death

Changes in metabolic activity of prostate cancer cells treated with Gamitrinibs or 17-AAG were determined by MTT, as described (12). For analysis of apoptosis, treated cells were analyzed for DEVDase (caspase) activity and plasma membrane integrity (propidium iodide, PI) using CaspaTag (Intergen, Burlington, MA), by multiparametric flow cytometry (12).

Superficial prostate cancer xenograft model

All experiments involving animals were approved by an Institutional Animal Care and Use Committee at the University of Massachusetts Medical School. For superficial prostate cancer xenografts, PC3 cells (5×10^6) were suspended in sterile PBS (200 μl) and injected subcutaneously into both flanks of 10 week-old CB17 SCID/beige (Taconic Farms) immunocompromised mice. When superficial tumors reached volumes of 100–150 mm^3, animals were randomized in four groups (2 tumors/mouse, 3 animals/group), and treated with vehicle (DMSO), G-TPP (10 mg/kg in 20% Cremophor EL) or 17-AAG (10 or 50 mg/kg in 20% Cremophor EL) by intraperitoneal (i.p.) injection. Tumor measurements were taken daily with a caliper, and tumor volume was calculated as described (16). Mice in the various treatment groups were weighed at the beginning and the end of each experiment.

Orthotopic bone metastatic prostate cancer model

PC3 cells (1×10^5) were injected in the medullar cavity of tibiae of immunocompromised CB17 SCID/beige mice according to published protocols (19). After 1 wk, animals (4/group) were started on vehicle (DMSO) or G-TPP (10 mg/kg) as daily i.p. injections for two additional wk. At the end of the experiment, mice in the various groups were sacrificed and their tibias were harvested, fixed in 4% paraformaldehyde for 4 d at 4°C, rinsed in PBS, pH 7.4, at −20°C, and bones were dehydrated in 50%–70% ethanol. Osteolysis in the various groups was first monitored by x-ray using a Faxitron soft X-ray machine, and quantified by micro-computed tomography (μCT).

μCT imaging

These experiments were carried out by the Musculoskeletal Center Imaging Core, University of Massachusetts Medical School using a Scanco Medical μCT 40 System (Bruttisellen, Switzerland). Scanning was carried out at 15 μm resolution in all three spatial dimensions (15 ×15 × 15 voxels) using a threshold range of 220–1000 to image mature bone. Morphometric properties were determined by analyzing the reconstructed slices for the region of bone from the growth plate to the fibular junction focusing on the region of tumor growth. Quantification of bone parameters, including bone volume, mean density and total volume was carried out by reformatting the μCT images of tibiae to the sagittal plane, and using a modified rectangle that contours the growth plate to the end of the hole area, excluding the subchondral bone. This same bone area was applied to the contralateral tibia for each mouse to obtain a percent of bone volume remaining in the tumor-bearing tibia compared to the normal limb. Axial sections reformatted to sagittal slices were used for calculations of bone volume (BV)/total bone (TB) of the area, and bone mineral density (BMD). BMD calculated values represent hydroxyapatite content per cm^3.

Histology

CB17/SCID mice carrying superficial PC3 xenograft tumors in the various groups were sacrificed, and organs, including brain, colon, heart, kidney, liver, lung, pancreas, small intestine, spleen, and stomach were collected, fixed in formalin and embedded in paraffin. Sections (5 μm) were put on high-adhesive slides, stained with hematoxylin and eosin (H&E) and analyzed histologically by light microscopy.

Statistical analysis

Data were analyzed using the unpaired t-test on a GraphPad software package (Prism 4.0) for Windows. All statistical tests were two sided. A *p*-value of 0.05 was considered to be statistically significant.

RESULTS

Activity of Gamitrinibs against prostate cancer cells

We began this study by testing the anticancer activity of mitochondria-targeted small molecule Hsp90 inhibitors, Gamitrinibs (16), in the NCI-60 cell line panel (http://dtp.nci.nih.gov/screening.html). In these experiments, increasing concentrations of Gamitrinib-G4 (G-G4) or Gamitrinib-TPP (G-TPP), which differ in the structure of their mitochondriotropic moiety (16), significantly inhibited tumor cell growth (Fig. 1A). Both compounds exhibited activity against all tumor types tested (Fig. 1A) with GI_{50} (concentrations that produced 50% inhibition of tumor growth) ranging between 4.62×10^{-7}–9.54×10^{-6} M for G-G4 and 1.6×10^{-7}–4.76×10^{-5} M for G-TPP. In this screening, both Gamitrinibs showed the highest GI_{50} activity against cell lines representative of colon cancer (G-G4, 7.68×10^{-7}–2.81×10^{-6} M; G-TPP, 3.59×10^{-7}–2.91×10^{-5} M), breast cancer (G-G4, 4.62×10^{-7}–2.64×10^{-6} M; G-TPP, 1.6×10^{-7}–3.38×10^{-6} M), and melanoma (G-G4, 4.89×10^{-7}–3.22×10^{-6} M; G-TPP, 3.61×10^{-7}–2.79×10^{-6} M) (Fig. 1A). Representative prostate cancer cells in this panel, PC3 and DU145 were also sensitive to Gamitrinibs, with GI_{50} concentrations of 1.31×10^{-6}–3.15×10^{-6} M for G-G4 and 1.72×10^{-6}–2.12×10^{-6} M for G-TPP.

Consistent with these findings, treatment with Gamitrinibs induced concentration-dependent loss of metabolic activity of androgen-independent and metastatic PC3 or C4-2B prostate cancer cells, by MTT (Fig. 1B). At the earliest time point tested (6 h), G-G2, G-G3 or G-G4 comparably inhibited metabolic activity of PC3 cells, whereas C4-2B cells were more sensitive to G-G-4 and G-TPP, compared to other Gamitrinibs (Fig. 1B, *left*). After a more prolonged, 24-h exposure, all Gamitrinib variants except G-G1 efficiently killed PC3 cells, while G-G1, G-G2 or G-G3 had intermediate activity against C4-2B cells (Fig. 1B, *right*). In contrast, comparable concentrations of 17-AAG had no effect on prostate cancer cell viability after 6 h, and only partial (25–50%) activity after a 24-h treatment (Fig. 1B). Consistent with genuine induction of apoptosis, treatment of PC3 cells with G-TPP for 24 h resulted in increased caspase activity and loss of plasma membrane integrity, by multiparametric flow cytometry, whereas 17-AAG had no effect within the same time interval (Fig. 1C). Mechanistically, PC3 cells treated with 17-AAG exhibited delayed, i.e. 24 h, reduced expression of cytosolic Akt, a known Hsp90 client protein (Fig. 1D), in agreement with previous data (14). In contrast, G-TPP treatment did not affect Akt levels in PC3 cells at any time point tested, consistent with the mitochondria-specific mechanism of action of these agents (Fig. 1D).

Acute mitochondrial permeability transition induced by Gamitrinibs in prostate cancer cells

Treatment of TMRM- and MitoTracker-labeled PC3 cells with G-TPP resulted in rapid and complete loss of mitochondrial membrane potential, by single-cell imaging and time-lapse videomicroscopy (Fig. 2A). Similarly, G-G4 or G-TPP induced immediate depolarization of

TMRM-labeled mitochondria isolated from PC3 cells (Fig. 2B). Pharmacologic inhibition of CypD peptidyl, prolyl *cis,trans* isomerase activity with CsA reversed mitochondrial depolarization induced by Gamitrinibs, whereas 17-AAG had no effect on mitochondrial membrane potential with or without CsA (Fig. 2B). In addition, G-TPP treatment of PC3-derived isolated mitochondria resulted in concentration-dependent release of cytochrome c in the supernatant (Fig. 2C). Consistent with a tumor-selective mechanism of action (16), G-TPP did not significantly affect cytochrome c content in mitochondria isolated from normal prostatic BPH-1 epithelial cells (Fig. 2C). In contrast, 17-AAG did not induce cytochrome c release from mitochondria of normal or tumor cell types (Fig. 2C).

To determine whether mitochondrial dysfunction induced by Gamitrinibs depended on Bcl-2 family members, we next simultaneously knocked down pro-apoptotic Bax and Bak molecules, which control outer membrane permeability (9). PC3 cells doubly transfected with Bax- and Bak-directed siRNA exhibited efficient knockdown of the intended target proteins, whereas a control, non-targeting siRNA was ineffective, by Western blotting (Fig. 2D). Under these conditions, treatment with G-TPP indistinguishably induced cytochrome c release (Fig. 2D) and loss of metabolic activity (Fig. 2E) in control transfectants or Bax/Bak knockdown PC3 cells.

Anticancer activity of Gamitrinibs in drug-resistant prostate cancer cells

Long-term culture of PC3 cells in the presence of 17-AAG induced resistance to 17-AAG-inhibition of metabolic activity, by MTT (Fig. 3A). These cells, designated PC3-GA, were also cross-resistant to taxol-induced cell death, as compared with parental, unselected PC3 cells (Fig. 3A). Resistant PC3-GA cells exhibited increased mRNA expression of the ABC transporter P-glycoprotein (P-gp), as compared with parental PC3 cells, whereas the levels of other membrane transporters implicated in drug efflux and resistance mechanisms, including ABCG2 and MRP1, were not affected (Fig. 3B). Similarly, the expression of cytoprotective chaperones, Hsp90, Hsp60, TRAP-1 or Hsp27, was unchanged in parental or PC3-GA cells, in the presence or absence of 17-AAG (Fig. 3C). Consistent with these observations, preincubation of PC3-GA cells with the pharmacologic inhibitor of P-gp, verapamil, partially restored their sensitivity to 17-AAG- or taxol-mediated anticancer activity (Fig. 3A). Under these conditions, G-G4 indistinguishably killed PC3 or PC3-GA cells, regardless of the presence of verapamil (Fig. 3D). Conversely, PC3-GA were resistant to G-TPP-dependent cell killing, in a response partially reversed by addition of verapamil (Fig. 3D).

Preclinical activity of Gamitrinibs in localized and bone metastatic prostate cancer

Systemic treatment of SCID/beige mice carrying established (~100–150 mm^3) s.c. PC3 xenograft tumors with vehicle or 17-AAG had no effect on exponential tumor growth, in vivo (Fig. 4A). In contrast, comparable concentrations of G-TPP (10 mg/kg as daily i.p. injections) completely inhibited PC3 tumor growth, in vivo (Fig. 4A). In concentration-dependent experiments, a dose of 17-AAG 5-fold higher than Gamitrinib (50 mg/kg as daily i.p. injections) was required to comparably inhibit PC3 tumor growth in mice (Fig. 4A). Animals in the various groups did not exhibit significant weight changes between the beginning and end of the various treatments (Fig. 4B). In addition, organs collected from vehicle- or G-TPP-treated animals were histologically unremarkable, with no appreciable difference in cellular morphology or tissue architecture (Fig. 4C).

Injection of PC3 cells in the tibiae of immunocompromised SCID/beige mice gave rise to extensive osteolytic lesions and bone loss over a 2-wk interval (Fig. 5A). Systemic administration of G-TPP to these animals significantly reduced bone loss within the same time interval, whereas vehicle (DMSO) was ineffective, by μCT analysis of isolated limbs (Fig. 5A). Quantification of μCT data under these conditions confirmed the extensive bone loss

associated with intratibial prostate cancer growth in DMSO-treated mice (Fig. 5B, *top*, *middle*), with significant reduction in total bone content in tibial tumor limb, compared to contralateral tibia (Fig. 5B, *bottom*). In all μCT analyses, G-TPP treated animals exhibited significant preservation of bone volume in tibial tumors compared to total bone volume (Fig. 5B, *top*, *middle*), or contralateral tibia (Fig. 5B, *bottom*).

Finally, treatment of PC3 cells with 17-AAG resulted in transient phosphorylation of the cell motility kinase, Src (Fig. 5C), which has been implicated in paradoxical enhanced metastatic dissemination during Hsp90-based therapy, in vivo (20). In contrast, PC3 cells treated with G-TPP showed no modulation of Src phosphorylation throughout a 24-h time interval (Fig. 5C), confirming the different mechanism of action of these agents, compared to 17-AAG. Total Src protein content was unchanged in G-TPP- or 17-AAG-treated cells (Fig. 5C)

DISCUSSION

In this study, we have shown that mitochondria-targeted Hsp90 inhibitors, Gamitrinibs (16) exert anticancer activity in models of drug-resistant, localized and bone metastatic prostate cancer, in vivo. Mechanistically, this pathway involves CypD-dependent mitochondrial permeability transition induced by Gamitrinibs, with sudden loss of organelle transmembrane potential, release of cytochrome c in the cytosol, and caspase-dependent apoptosis. Systemic administration of Gamitrinibs to mice was well tolerated, and devoid of significant systemic or organ toxicity, in vivo. Compared to non-subcellularly directed Hsp90 therapy, i.e. 17-AAG, Gamitrinibs do not affect chaperone client protein stability in the cytosol, or Src phosphorylation, and exhibit at least a five-fold greater potency for inhibition of xenograft tumor growth, in vivo.

One of the invariable features of advanced and metastatic prostate cancer is an elevated anti-apoptotic threshold, which contributes to disease progression (21). Although much work has focused on the role of Bcl-2 (9) or Inhibitor of Apoptosis (IAP) (22) proteins in this process, recent data have suggested the existence of “mitochondrial-intrinsic” cytoprotective mechanisms, including the recruitment of Hsp90 chaperones to the organelle matrix, and their ability to antagonize CypD-dependent permeability transition (12). As selective inhibitors of this pathway, Gamitrinibs displayed here anticancer activity across the spectrum of the NCI 60-cell line panel, suggesting that cytoprotection by mitochondrial Hsp90s (12) is broadly exploited in genetically heterogeneous tumor types. Consistent with this model, Gamitrinibs functioned as direct “mitochondriotoxic” agents, inducing acute organelle dysfunction in prostate cancer cells (13). Importantly, this response was independent of pro-apoptotic Bcl-2 family proteins, Bax and Bak, which are considered essential ‘gatekeepers’ for many mitochondrial cell death stimuli (23), and regulate apoptotic responses to chemopreventive (24) or therapeutic (25) agents in prostate cancer. Mechanistically, the independence of Gamitrinib-mediated cell killing from pro-apoptotic Bcl-2 proteins may reflect their direct activation of CypD-dependent mitochondrial permeability transition, which may ultimately result in swelling of the matrix and rupture of the organelle outer membrane.

The molecular underpinnings of how Hsp90 chaperones control a CypD (12)-regulated permeability transition pore (7) remains to be fully elucidated. Drawing from other experimental models, this pathway has been implicated in inhibition of oxidative stress-induced apoptosis (26,27), potentially via activating phosphorylation by the mitochondrial kinase, PINK1 (28). This is in keeping with an essential role of CypD in oxidative stress-induced mitochondrial dysfunction (29,30), suggesting that cytoprotection by mitochondrial Hsp90s may be ideally suited to enhance tumor adaptability to unfavorable microenvironments (31), rich in reactive oxygen species (32), for instance metastatic sites, in vivo (33).

In this context, systemic administration of Gamitrinibs prevented bone destruction and preserved bone volume in an orthotopic model of intraosseous prostate cancer growth (19). Bone metastatic prostate cancer is a life-threatening hallmark of advanced disease (34), and is mechanistically contributed by a complex interplay between tumor cells, osteoblasts and osteoclasts, multiple mediators of the tumor microenvironment, including low pH, hypoxia, high Ca^{2+} concentrations (35), and growth factor signaling (36). The management of bone metastatic prostate cancer is largely palliative (33), and the utility of Hsp90-based therapy in these settings is controversial, as 17-AAG paradoxically exacerbated metastatic dissemination, in vivo (37), potentially via transient Src activation (20). In contrast, Gamitrinib had no effect on Src activation, reinforcing its distinct mechanism of action compared to non-subcellularly targeted Hsp90 antagonists. How AR signaling participates in bone metastatic prostate cancer has remained controversial, and whether this pathway is required for osteoblastic lesion formation in patients with advanced disease has not been elucidated (36). On the other hand, Gamitrinibs indistinguishably killed AR-dependent or –independent prostate cancer cell types (13), reinforcing their potential suitability for bone anti-metastatic regimens.

A second common feature of advanced prostate cancer is resistance to therapy, and this response is often due to acquired upregulation of ABC transporters via different mechanisms, including demethylation of the CpG-containing promoter of the Multiple Drug Resistance-1 (MDR-1) gene (38), increased P-gp expression (38), or oligomerization of BCRP/ABCG2 (39). Here, protracted exposure of PC3 cells to 17-AAG, i.e. PC3-GA cells, selectively upregulated the expression of P-gp (40), whereas other ABC transporters or various cytoprotective chaperones implicated in drug resistance mechanisms in prostate cancer (41) were not affected. Although resistant to 17-AAG, and cross-resistant to taxol, PC3-GA cells remained fully sensitive to Gamitrinib-G4-mediated cell killing, but not Gamitrinib-TPP, suggesting that the presence of distinct “mitochondriotropic” moieties (12) may influence Gamitrinib metabolism and drug efflux.

In summary, the preclinical data reported here identify Gamitrinibs (16) as promising anticancer agents for advanced prostate cancer, in vivo. Although Hsp90 has been pursued as a promising nodal target for cancer drug discovery (14), the clinical experience with Hsp90-directed therapy (15) has so far been modest, inferior to the expectations of pathway inhibition as a strategy to overcome tumor heterogeneity (42). Together with recent work (13), the data presented here reinforce the importance of Hsp90 as a global cancer drug target (14), but also underscore that the subcellular compartmentalization of the chaperone to mitochondria (12) plays a pivotal role in tumor maintenance, and may ultimately dictate the clinical success of Hsp90 therapeutics in humans (16). In this context, the broad anticancer activity of Gamitrinibs (16), including in models of metastatic and multidrug-resistant prostate cancer (this study), reinforces the feasibility of mitochondria-targeted drug discovery for novel anticancer strategies (10).

STATEMENT OF TRANSLATIONAL RELEVANCE

The molecular chaperone Heat Shock Protein-90 (Hsp90) is a “nodal” target for cancer therapy, orchestrating multiple pathways of tumor cell proliferation, survival and adaptation. Although feasible, current Hsp90-based therapy has shown so far modest activity in the clinic, inferior to the expectations of multiple pathway inhibition. This may reflect the existence of a protective pool of Hsp90 compartmentalized in mitochondria of tumor cells, which is not inhibited by current antagonists. In this study, we tested the activity of a novel class of mitochondria-targeted, small molecule Hsp90 inhibitors, Gamitrinibs (GA mitochondrial matrix inhibitors) in preclinical models of advanced prostate cancer, a condition in urgent need of fresh therapeutic advances. Here, Gamitrinibs acted as direct “mitochondriotoxic” agents, inducing acute organelle dysfunction, apoptosis and killing of

hormone-refractory, metastatic and multidrug-resistant prostate cancer cells. Systemic administration of Gamitrinibs to mice was well tolerated, and inhibited localized or bone metastatic prostate cancer growth without organ or tissue toxicity, in vivo. Therefore, selective inhibition of mitochondrial Hsp90 activity by Gamitrinibs may provide new therapeutic approaches for advanced prostate cancer in humans.

Acknowledgments

GRANT SUPPORT

This work was supported by National Institutes of Health grants CA140043 (DCA, LRL, JBL, GSS), HL54131, CA78810, and CA118005 (DCA), CA82834 (GSS), and Deutsche Forschungsgemeinschaft grant, Si 1546/1-1 (MDS).

REFERENCES

1. Carter HB, Ferrucci L, Kettermann A, et al. Detection of life-threatening prostate cancer with prostate-specific antigen velocity during a window of curability. J Natl Cancer Inst 2006;98:1521–1527. [PubMed: 17077354]
2. Taichman RS, Loberg RD, Mehra R, Pienta KJ. The evolving biology and treatment of prostate cancer. J Clin Invest 2007;117:2351–2361. [PubMed: 17786228]
3. Vogiatzi P, Cassone M, Claudio L, Claudio PP. Targeted therapy for advanced prostate cancer: Looking through new lenses. Drug News Perspect 2009;22:593–601. [PubMed: 20140279]
4. Chen CD, Welsbie DS, Tran C, et al. Molecular determinants of resistance to antiandrogen therapy. Nat Med 2004;10:33–39. [PubMed: 14702632]
5. Danial NN, Korsmeyer SJ. Cell death: critical control points. Cell 2004;116:205–219. [PubMed: 14744432]
6. Bouchier-Hayes L, Lartigue L, Newmeyer DD. Mitochondria: pharmacological manipulation of cell death. J Clin Invest 2005;115:2640–2647. [PubMed: 16200197]
7. Green DR, Kroemer G. The pathophysiology of mitochondrial cell death. Science 2004;305:626–629. [PubMed: 15286356]
8. Fesik SW. Promoting apoptosis as a strategy for cancer drug discovery. Nat Rev Cancer 2005;5:876–885. [PubMed: 16239906]
9. Chipuk JE, Moldoveanu T, Llambi F, Parsons MJ, Green DR. The BCL-2 family reunion. Mol Cell 2010;37:299–310. [PubMed: 20159550]
10. Fulda S, Galluzzi L, Kroemer G. Targeting mitochondria for cancer therapy. Nat Rev Drug Discov 2010;9:447–464. [PubMed: 20467424]
11. Whitesell L, Lindquist SL. HSP90 and the chaperoning of cancer. Nat Rev Cancer 2005;5:761–772. [PubMed: 16175177]
12. Kang BH, Plescia J, Dohi T, Rosa J, Doxsey SJ, Altieri DC. Regulation of tumor cell mitochondrial homeostasis by an organelle-specific Hsp90 chaperone network. Cell 2007;131:257–270. [PubMed: 17956728]
13. Leav I, Plescia J, Goel HL, et al. Cytoprotective mitochondrial chaperone TRAP-1 as a novel molecular target in localized and metastatic prostate cancer. Am J Pathol 2010;176:393–401. [PubMed: 19948822]
14. Isaacs JS, Xu W, Neckers L. Heat shock protein 90 as a molecular target for cancer therapeutics. Cancer Cell 2003;3:213–217. [PubMed: 12676580]
15. Drysdale MJ, Brough PA. Medicinal chemistry of Hsp90 inhibitors. Curr Top Med Chem 2008;8:859–868. [PubMed: 18673171]
16. Kang BH, Plescia J, Song HY, et al. Combinatorial drug design targeting multiple cancer signaling networks controlled by mitochondrial Hsp90. J Clin Invest 2009;119:454–464. [PubMed: 19229106]
17. Thalmann GN, Anezinis PE, Chang SM, et al. Androgen-independent cancer progression and bone metastasis in the LNCaP model of human prostate cancer. Cancer Res 1994;54:2577–2581. [PubMed: 8168083]

18. Dohi T, Beltrami E, Wall NR, Plescia J, Altieri DC. Mitochondrial survivin inhibits apoptosis and promotes tumorigenesis. J Clin Invest 2004;114:1117–1127. [PubMed: 15489959]
19. Akech J, Wixted JJ, Bedard K, et al. Runx2 association with progression of prostate cancer in patients: mechanisms mediating bone osteolysis and osteoblastic metastatic lesions. Oncogene 2009;29:811–821. [PubMed: 19915614]
20. Yano A, Tsutsumi S, Soga S, et al. Inhibition of Hsp90 activates osteoclast c-Src signaling and promotes growth of prostate carcinoma cells in bone. Proc Natl Acad Sci U S A 2008;105:15541–15546. [PubMed: 18840695]
21. Huang X, Zhang X, Farahvash B, Olumi AF. Novel targeted pro-apoptotic agents for the treatment of prostate cancer. J Urol 2007;178:1846–1854. [PubMed: 17868738]
22. Srinivasula SM, Ashwell JD. IAPs: what's in a name? Mol Cell 2008;30:123–135. [PubMed: 18439892]
23. Wei MC, Zong W-X, Cheng EHY, et al. Proapoptotic BAX and BAK: A Requisite Gateway to Mitochondrial Dysfunction and Death. Science 2001;292:727–730. [PubMed: 11326099]
24. Hahm E-R, Arlotti JA, Marynowski SW, Singh SV. Honokiol, a Constituent of Oriental Medicinal Herb Magnolia officinalis, Inhibits Growth of PC-3 Xenografts In vivo in Association with Apoptosis Induction. Clinical Cancer Research 2008;14:1248–1257. [PubMed: 18281560]
25. Shankar S, Ganapathy S, Srivastava RK. Sulforaphane Enhances the Therapeutic Potential of TRAIL in Prostate Cancer Orthotopic Model through Regulation of Apoptosis, Metastasis, and Angiogenesis. Clinical Cancer Research 2008;14:6855–6866. [PubMed: 18980980]
26. Hua G, Zhang Q, Fan Z. Heat shock protein 75 (TRAP1) antagonizes reactive oxygen species generation and protects cells from granzyme M-mediated apoptosis. J Biol Chem 2007;282:20553–20560. [PubMed: 17513296]
27. Montesano Gesualdi N, Chirico G, Pirozzi G, Costantino E, Landriscina M, Esposito F. Tumor necrosis factor-associated protein 1 (TRAP-1) protects cells from oxidative stress and apoptosis. Stress 2007;10:342–350. [PubMed: 17853063]
28. Pridgeon JW, Olzmann JA, Chin LS, Li L. PINK1 Protects against Oxidative Stress by Phosphorylating Mitochondrial Chaperone TRAP1. PLoS Biol 2007;5:e172. [PubMed: 17579517]
29. Baines CP, Kaiser RA, Purcell NH, et al. Loss of cyclophilin D reveals a critical role for mitochondrial permeability transition in cell death. Nature 2005;434:658–662. [PubMed: 15800627]
30. Nakagawa T, Shimizu S, Watanabe T, et al. Cyclophilin D-dependent mitochondrial permeability transition regulates some necrotic but not apoptotic cell death. Nature 2005;434:652–658. [PubMed: 15800626]
31. Karl TB, Helen OM, Andrea D, et al. Hypoxia selects for androgen independent LNCaP cells with a more malignant geno- and phenotype. International Journal of Cancer 2008;123:760–768.
32. Sung S-Y, Hsieh C-L, Law A, et al. Coevolution of Prostate Cancer and Bone Stroma in Three-Dimensional Coculture: Implications for Cancer Growth and Metastasis. Cancer Res 2008;68:9996–10003. [PubMed: 19047182]
33. Mundy GR. Metastasis to bone: causes, consequences and therapeutic opportunities. Nat Rev Cancer 2002;2:584–593. [PubMed: 12154351]
34. Roodman GD. Mechanisms of bone metastasis. N Engl J Med 2004;350:1655–1664. [PubMed: 15084698]
35. Guise TA, Mohammad KS, Clines G, et al. Basic mechanisms responsible for osteolytic and osteoblastic bone metastases. Clin Cancer Res 2006;12:6213s–6216s. [PubMed: 17062703]
36. Li ZG, Mathew P, Yang J, et al. Androgen receptor-negative human prostate cancer cells induce osteogenesis in mice through FGF9-mediated mechanisms. J Clin Invest 2008;118:2697–2710. [PubMed: 18618013]
37. Price JT, Quinn JM, Sims NA, et al. The heat shock protein 90 inhibitor, 17-allylamino-17-demethoxygeldanamycin, enhances osteoclast formation and potentiates bone metastasis of a human breast cancer cell line. Cancer Res 2005;65:4929–4938. [PubMed: 15930315]
38. Takeda M, Mizokami A, Mamiya K, et al. The establishment of two paclitaxel-resistant prostate cancer cell lines and the mechanisms of paclitaxel resistance with two cell lines. Prostate 2007;67:955–967. [PubMed: 17440963]

39. Xie Y, Xu K, Linn DE, et al. The 44-kDa Pim-1 kinase phosphorylates BCRP/ABCG2 and thereby promotes its multimerization and drug-resistant activity in human prostate cancer cells. J Biol Chem 2008;283:3349–3356. [PubMed: 18056989]

40. Sánchez C, Mendoza P, Contreras HR, et al. Expression of multidrug resistance proteins in prostate cancer is related with cell sensitivity to chemotherapeutic drugs. The Prostate 2009;69:1448–1459. [PubMed: 19496068]

41. Andrieu C, Taieb D, Baylot V, et al. Heat shock protein 27 confers resistance to androgen ablation and chemotherapy in prostate cancer cells through eIF4E. Oncogene 2010;29:1883–1896. [PubMed: 20101233]

42. Butcher EC. Can cell systems biology rescue drug discovery? Nat Rev Drug Discov 2005;4:461–467. [PubMed: 15915152]

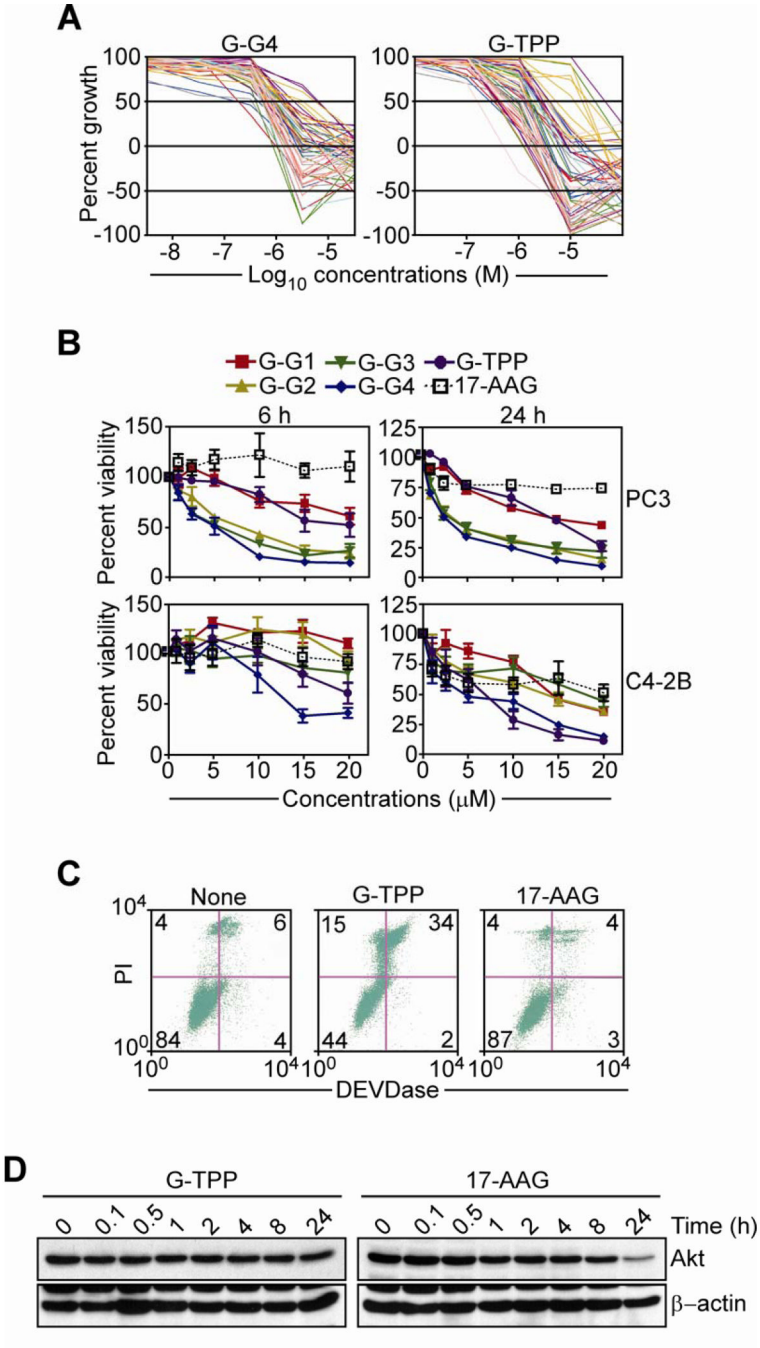

Figure 1. Anticancer activity of Gamitrinibs

A, Gamitrinib-G4 (G-G4) or Gamitrinib-TPP (G-TPP) were analyzed for inhibition of cell proliferation in a NCI 60-cell line screening by MTT. Each line corresponds to a different tumor cell type. B, Prostate cancer PC3 (*top*) or C4-2B (*bottom*) cells were incubated with the indicated increasing concentrations of Gamitrinibs (G1–G4, G-TPP) or 17-AAG and analyzed after 6 h (*left*) or 24 h (*right*), by MTT. Mean±SEM of replicates. C, PC3 cells were incubated with G-TPP or 17-AAG, and analyzed for DEVDase (caspase) activity and propidium iodide (PI) staining by multiparametric flow cytometry. The percentage of cells in each quadrant is indicated. None, untreated. D, PC3 cells were treated with G-TPP or 17-AAG for the indicated time intervals, and analyzed by Western blotting.

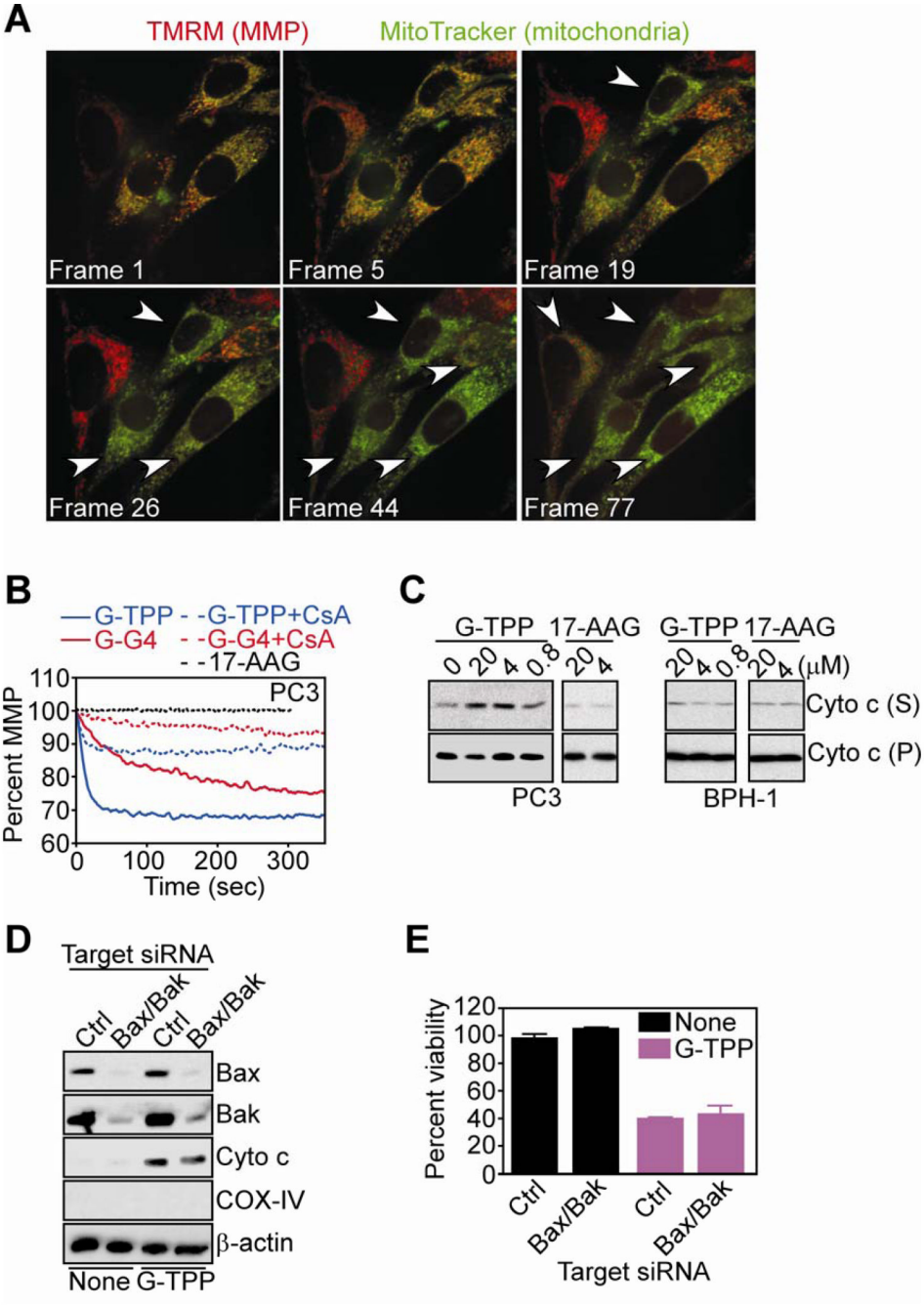

Figure 2. Mitochondriotoxic mechanism of action of Gamitrinibs in prostate cancer cells

A, PC3 cells were double-labeled with TMRM (red fluorescence, mitochondrial membrane potential, MMP) and MitoTracker (green fluorescence, mitochondria), treated with G-TPP and analyzed by time-lapse videomicroscopy. Representative sequential images after treatment are shown. 1 frame = 5 min. *Arrowheads*, PC3 cells that have lost MMP. B, TMRM-labeled mitochondria isolated from PC3 cells were incubated with 17-AAG, G-TPP or G-G4 in the presence or absence of CSA, and analyzed for changes in mitochondrial membrane potential in a fluorimeter. C, Mitochondria from PC3 or normal prostatic epithelial BPH-1 cells were treated with 17-AAG or G-TPP, and analyzed for cytochrome c content in pellets (P) or supernatants (S). D, PC3 cells were transfected with control (Ctrl) non-targeting or Bax and

Bak-directed siRNA, and analyzed by Western blotting. None, untreated. E, siRNA transfected PC3 cells were treated as indicated and analyzed by MTT. Mean±SEM of replicates.

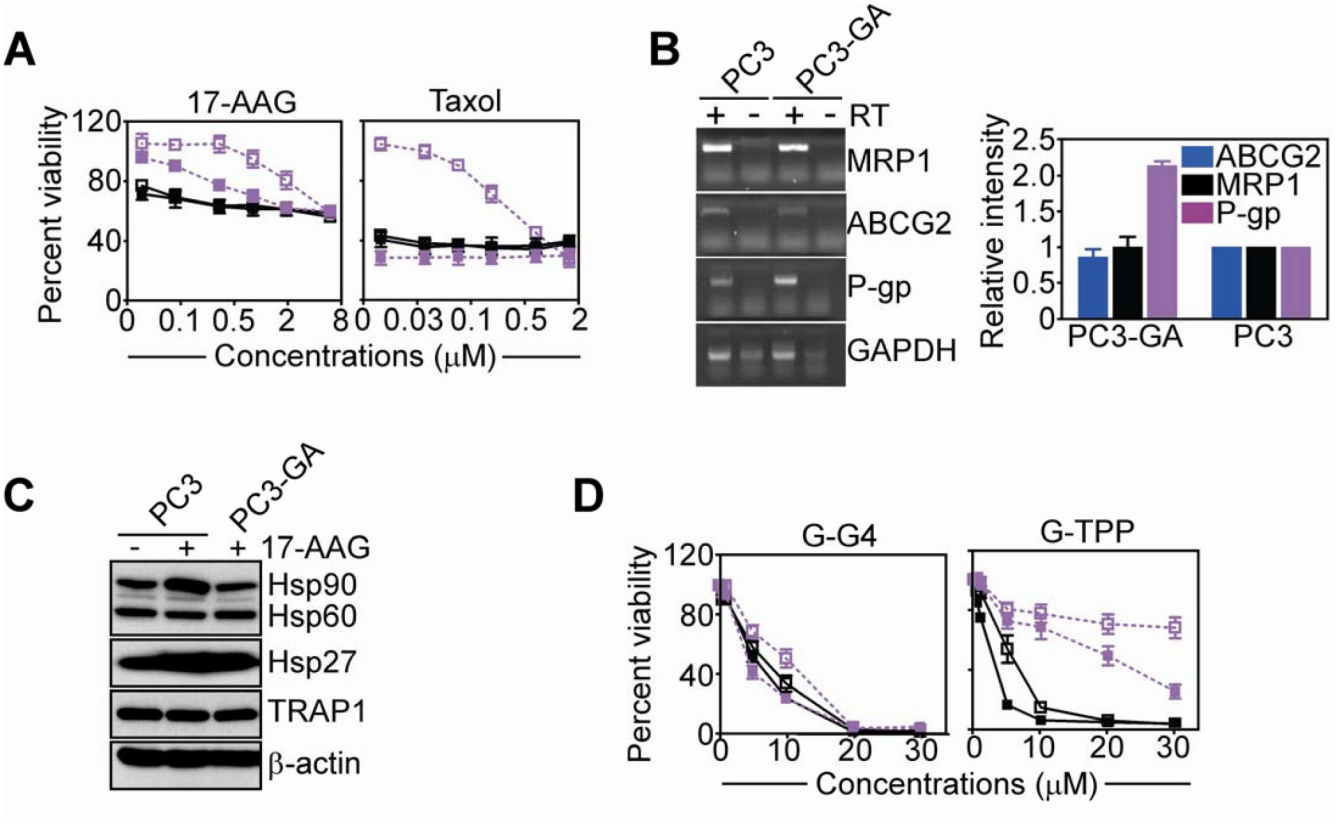

Figure 3. Activity of Gamitrinib against multidrug-resistant prostate cancer

A, PC3 (*black*) or PC3-GA (*purple*) cells were treated with the indicated concentrations of 17-AAG (*left*) or taxol (*right*), and analyzed by MTT in the presence (*solid symbols*) or absence (*open symbols*) of verapamil (20 μM). B, PC3 or PC3-GA cells were analyzed by PCR, and amplified bands were visualized by ethidium bromide staining (*left*), and quantified (*right*). RT, reverse transcriptase. C, PC3 or PC3-GA cells were analyzed by Western blotting before or after treatment with 17-AAG. D, The experimental conditions are as in A, except that PC3 or PC3-GA cells were treated with G-G4 (*left*) or G-TPP (*right*) and analyzed by MTT. For panels, A, B and D, mean±SEM of replicates.

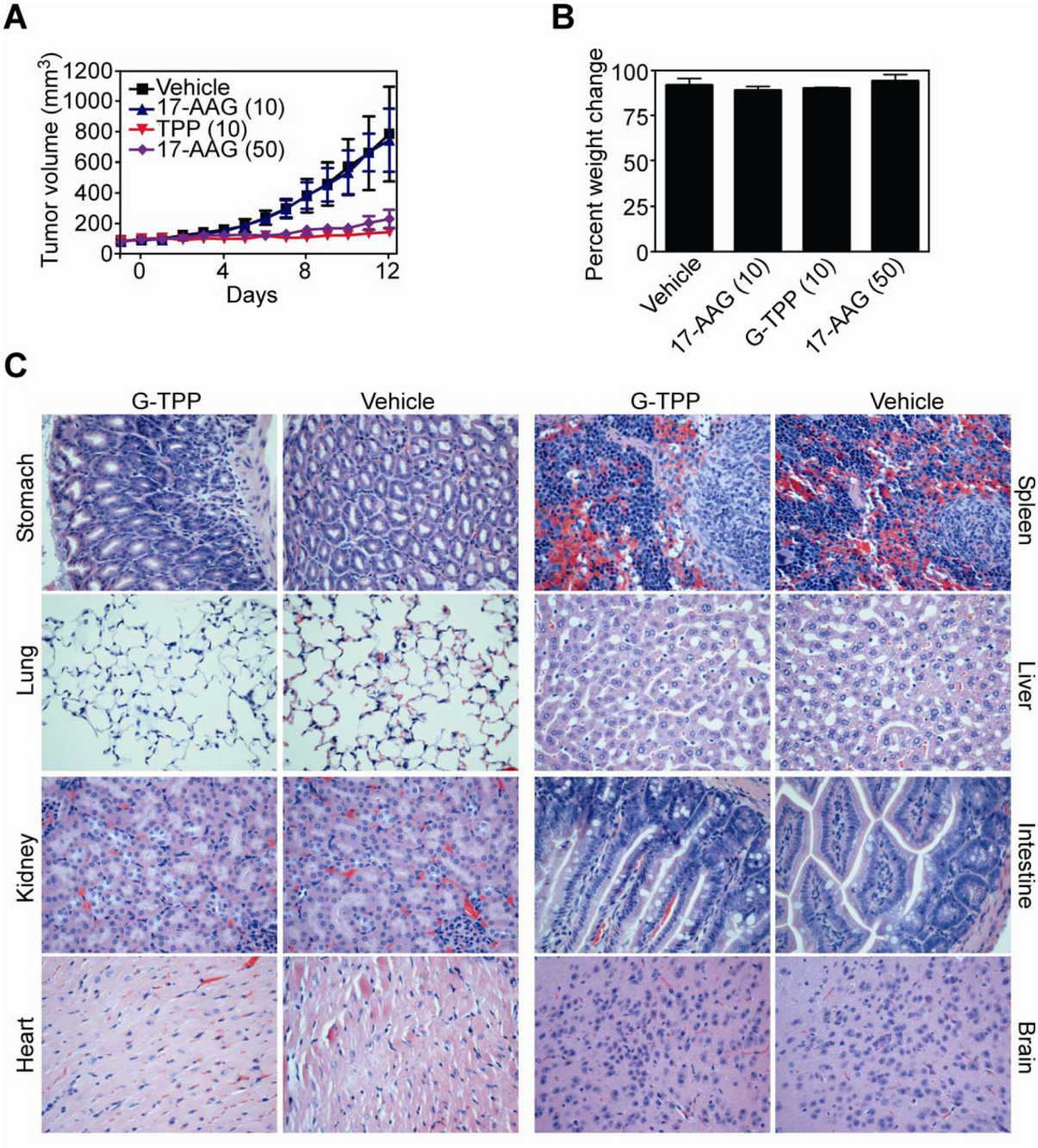

Figure 4. Activity of Gamitrinib in localized prostate cancer, in vivo

A, CB17 SCID/beige mice carrying established PC3 superficial tumors (100–150 mm^3) were treated systemically with G-TPP or 17-AAG and tumor volume was determined with a caliper. Numbers in parentheses correspond to the concentrations used in mg/kg. Vehicle, DMSO-treated group. Mean±SEM of the various groups. B, Mice in the various treatment groups were weighed at the beginning and end of the experiment, and analyzed for percent weight change. Numbers in parentheses correspond to the concentrations used (mg/kg). C, The indicated organs harvested from representative mice in the G-TPP or vehicle group were stained with H&E and analyzed by light microscopy. Magnification, ×100.

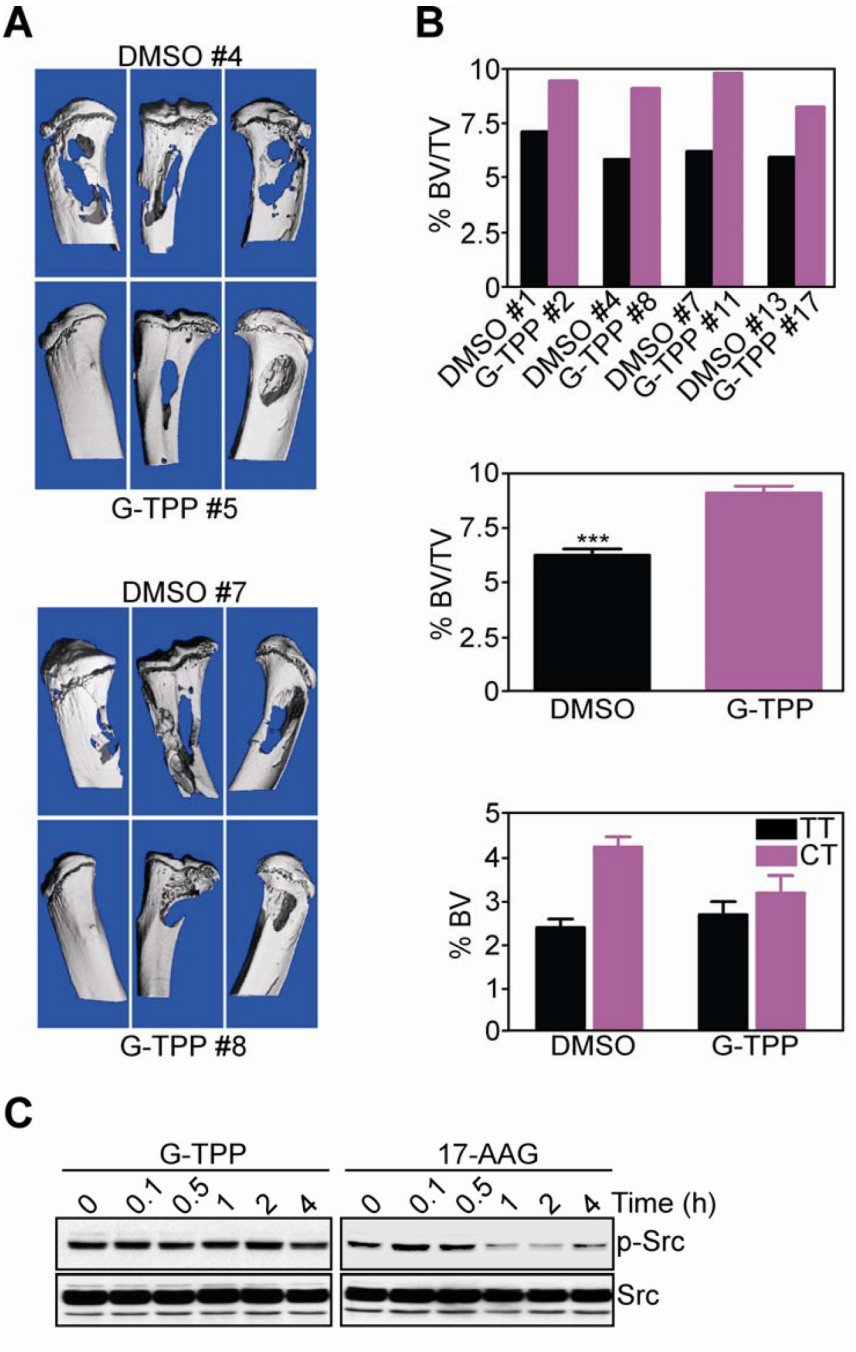

Figure 5. Activity of Gamitrinib in an orthotopic model of bone metastatic prostate cancer

A, CB17 SCID/beige mice injected in the tibiae with PC3 cells were treated with G-TPP or vehicle (DMSO), and limbs of representative animals in each group (#) were analyzed by μCT. B, Percent change in bone volume (BV)/total volume (TV) ratio in individual animals (*top*) or groups (*middle*) treated with DMSO or G-TPP, as determined by μCT reconstruction of bone lesions. *Bottom*, percent BV of tibial tumor limb (TT) or contralateral tibia (CT). Mean±SEM of individual determinations. C, PC3 cells were treated with G-TPP or 17-AAG for the indicated time intervals, and analyzed by Western blotting.